Presented at the 1977
Intern. Symposium on
Lepton and Photon
Interactions at High
Energies - Hamburg,
August 25-31, 1977

ISTITUTO NAZIONALE DI FISICA NUCLEARE
Laboratori Nazionali di Frascati

LNF-77/51(P)
25 Ottobre 1977

C. Bemporad: RECENT RESULTS AT ADONE.

Servizio Documentazione
dei Laboratori Nazionali di Frascati

RECENT RESULTS AT ADONE

C. Bemporad
Laboratori Nazionali dell'INFN, Frascati, Italia
Istituto di Fisica dell'Università di Pisa, and
Istituto Nazionale di Fisica Nucleare, Sezione di Pisa, Italia

## ABSTRACT

A review is given of the new structures which were recently identified in the C. M. energy interval between 1.4 and 2.2 GeV.

The experimental results were obtained by the three groups operating at ADONE: $B\bar{B}$, $\gamma\gamma 2$, MEA[1].

## I INTRODUCTION

In preparing this paper I went back to the 1975 Stanford Symposium Proceedings to give a look to the Symposium summary and prognosis by Bjorken[2]. Most of his talk was naturally centered on the new physics of the $J/\psi$, $\psi'$, etc. but it also pointed out how the energy region between the $\varphi$ and the $J/\psi$ might reserve surprises to a more careful investigation and perhaps new important discoveries. It also contained a pictorial representation of what might happen during experimentation (Fig. 1). Apart from some excessive optimism about the time schedule, it is now clear

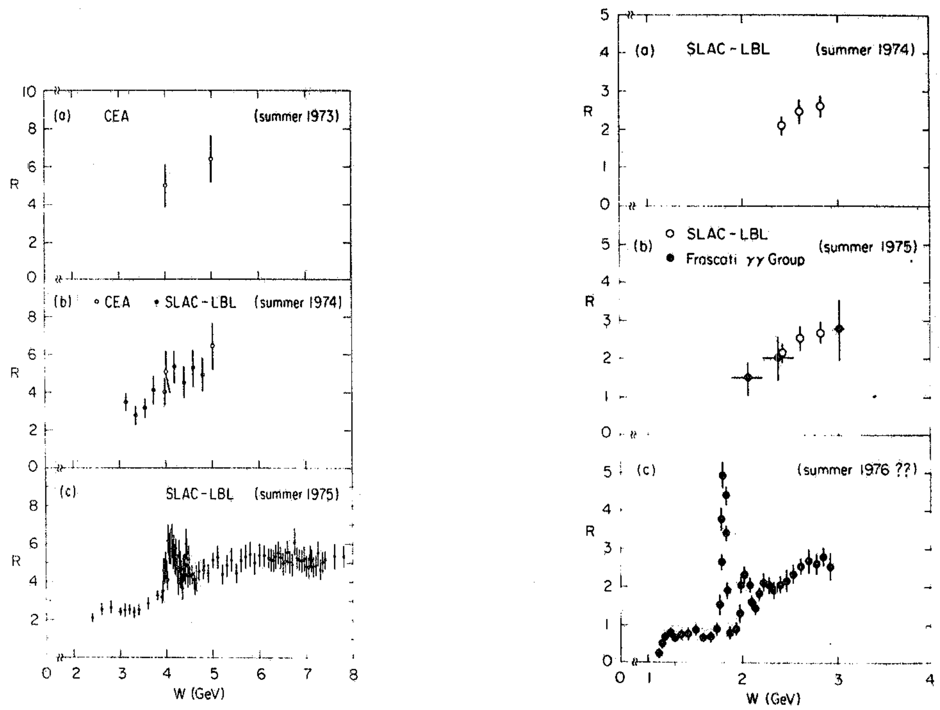


Fig. 1 J.D. Bjorken's 1975 predictions on the evolution of knowledge in $e^+e^-$ physics at center of mass energies lower than 3 GeV.

that an accurate energy scanning reveals a striking complexity of the hadron production in the low energy domain covered by ADONE and the new french machine DCI.

I shall review the subject following a more or less historical line and discussing the resonances present in the energy regions around 2.1, 1.8 and 1.5 GeV. At the lower energy, the data taking will go on for several extra months and the preliminary results presented here should be considerably improved.

## II GENERALITIES ON ADONE EXPERIMENTS

I shall give only the main characteristics of the $B\bar{B}$, $\gamma\gamma 2$ and MEA experiments. They are positioned in three of the four ADONE interaction regions (Fig. 2); the fourth interaction region, opposite to the $B\bar{B}$ experiment, contains a small angle Bhabha scattering luminosity monitor.

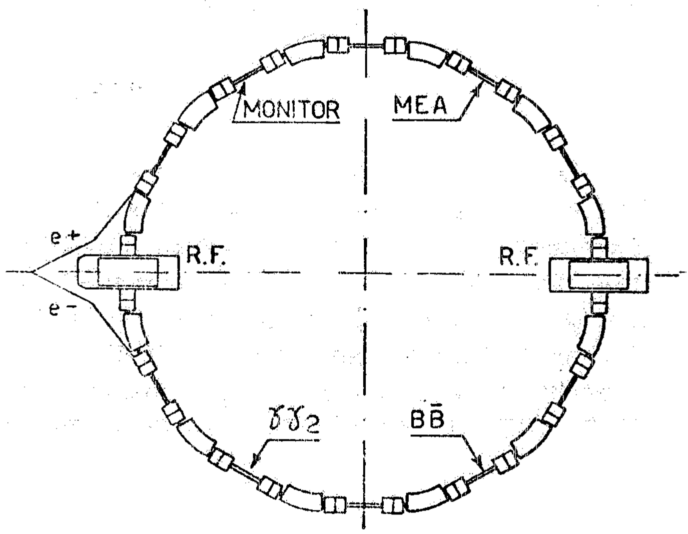


Fig. 2 Sketch of ADONE with positions of the $B\bar{B}$, $\gamma\gamma 2$, MEA experiments and of the small angle Bhabha scattering monitor.

The energy spread (f. w. h. m.) of the machine is given by the expression

$$\Gamma_W(\mathrm{MeV}) = 0.32\ W^2\ (\mathrm{GeV})\ .$$

In the 1.4-2.0 GeV energy interval, the source length (f. w. h. m.) at the interaction regions has a $\Gamma$ varying between 25 and 45 cm. The absolute value of the machine energy is known with an uncertainty of $\Delta W = \pm 2$ MeV. The average luminosity delivered by ADONE at a C. M. energy W of 1.5 GeV is about 1 $nb^{-1}$/day. The three experiments have somewhat complementary properties; these are summarized in Table I.

### 1. The $B\bar{B}$ experiment

The $B\bar{B}$ set-up has a cylindrical symmetry around the interaction region of the $e^+e^-$ beams and it covers a solid angle for point like source (f. p. l. s.) of $0.7 \times 4\pi$ sr (Fig. 3).

The system is composed of four coaxial hodoscopes (from the interaction region outward: HOD 1, HOD 2, HOD 3, HOD 4), each made up of sixteen scintillation counter elements.

All counters respond linearly to the energy loss of the detected particles. The HOD 3 elements are thick liquid scintillation counters (35 g/cm$^2$ and 0.8 R. L.); they effectively discriminate crossing particles from soft

# TABLE I

## Main properties of Adone experiments

$B\bar{B}$ Calorimetry; dE/dx vs. E - $\gamma\gamma 2$ $\gamma$ detection - MEA Momentum analysis

| | $B\bar{B}$ | $\gamma\gamma 2$ | MEA |
|---|---|---|---|
| Orientation of the axis of symmetry referred to the beam direction | parallel | orthogonal | orthogonal |
| Solid angle for point like source /$4\pi$ | 70 % | 66 (40) % | 40 % |
| Direction measured by | magnetostrictive S. C. | optical S. C. | optical S. C. |
| Momentum measured by | E, dE/dx | range | magnet |
| Quality of mom. meas. | poor | poor | good |
| Quality of photon detection | poor | good | poor |
| Minimum energy (MeV) for a pion to trigger | $\sim$ 60 | $\sim$ 120 ($\sim$ 35 + $\gamma$'s) | $\sim$ 130 |
| Luminosity monitors | S. A. Bhabha<br>W. A. Bhabha<br>Double bremss. | S. A. Bhabha<br>W. A. Bhabha | S. A. Bhabha<br>W. A. Bhabha |

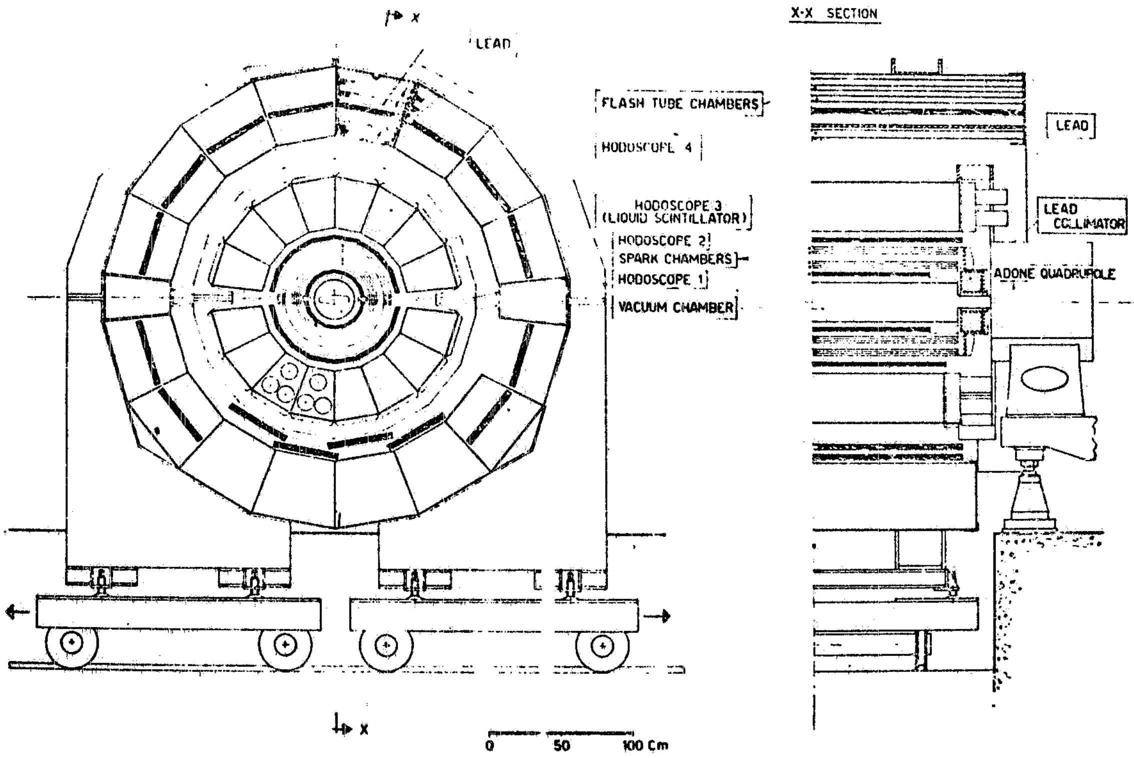


Fig. 3 The $B\bar{B}$ experimental apparatus.

electromagnetic background by means of a "calorimetric" information ($\Gamma_E/E \sim 20\,\%$ at E = 100 MeV). Twelve of the sixteen HOD 4 elements are separated from HOD 3 by 2.5 R.L. of iron-lead radiator.

Four cylindrical magnetostrictive wire chambers track charged particles between HOD 1 and HOD 2.

A set of flash tube chambers, with tubes parallel to the $e^+e^-$ beams and arranged into two double gaps, is placed in front and behind of HOD 4 and the lead radiator. The chamber system is interfaced by fiber optics to an automatic vidicon readout. HOD 4, the iron-lead radiator, the flash tube chambers provide electron identification and form a rough photon detector (some photon conversion occurs also in HOD 3).

The trigger logic allows the selection of parallel and different trigger conditions to enable the data acquisition. The pattern of the fired counters, their pulse height and time information, the information from the spark and flash tube chambers, are all recorded on magnetic tape for each event. A track is defined by elements of HOD 1, 2, 3 set in a row; the minimum energy for a pion track to trigger is $T_\pi \sim 60$ MeV; at least two tracks are requested.

## 2. The $\gamma\gamma 2$ experiment

The apparatus consists of two large semicylindrical telescopes, placed above and below the interaction region, with their axes orthogonal to the $e^+e^-$ beams (Fig. 4).

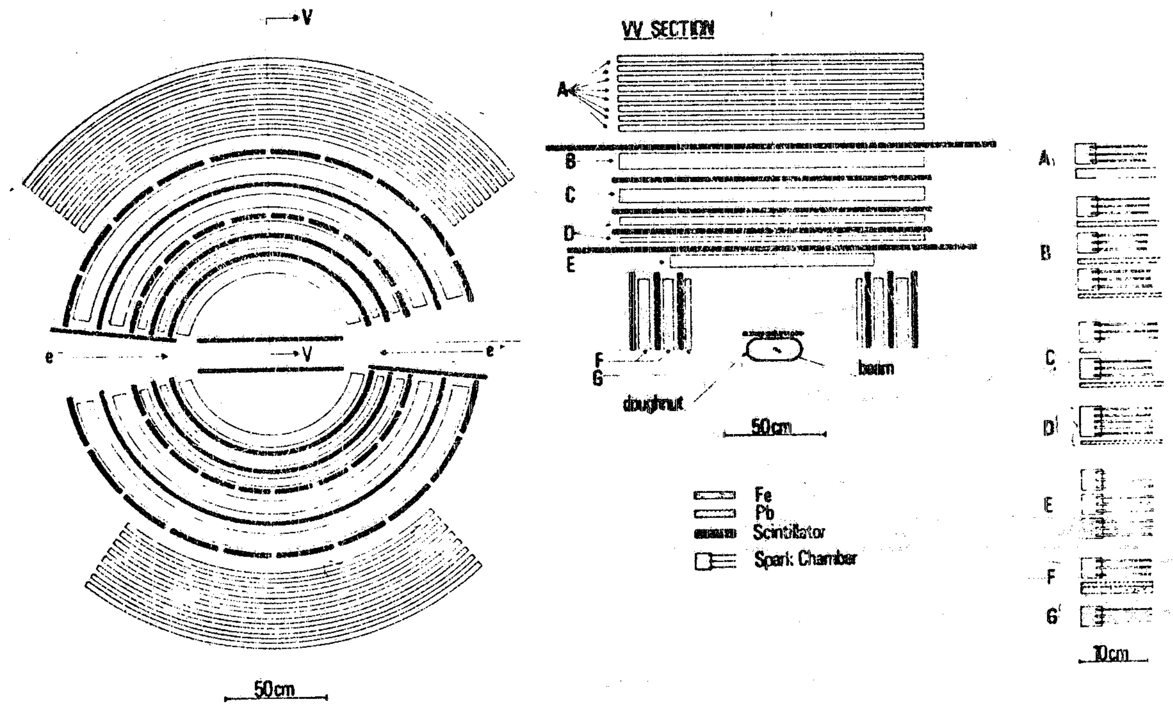


Fig. 4 The $\gamma\gamma 2$ experimental apparatus.

The telescopes are made of a combination of scintillation counters, optical spark chambers and lead converters arranged in such a way as to optimize the electromagnetic shower detection. The solid angle f.p. l.s. is $0.41 \times 4\pi$ sr. for triggering and $0.66 \times 4\pi$ sr. for tracking. The total thickness of the shower detector is 5.5 R.L.; the photon detection efficiency is shown in Fig. 5 as a function of the photon energy.

The shower detector is completed by the addition of a set of eight bigap spark chambers sandwiched between nine 1.5 cm thick iron layers and covering a solid angle of $0.27 \times 4\pi$ sr. The total thickness of the apparatus corresponds to the range of a 300 MeV pion.

A pair of circular side-telescopes made of magnetostrictive spark chambers, lead absorbers and scintillation counters complete the detection system and cover an additional solid angle of $0.15 \times 4\pi$ sr.

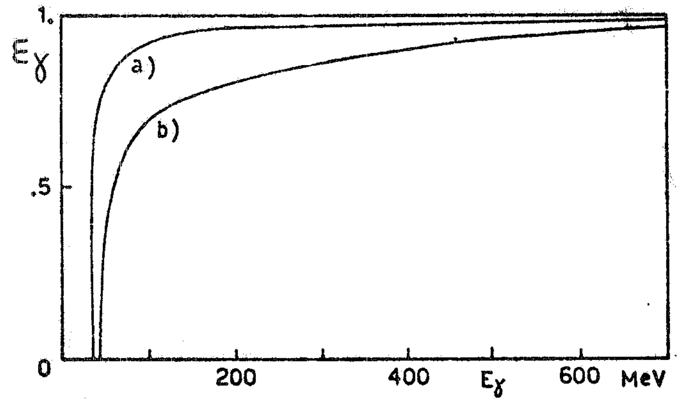


Fig. 5 Photon detection efficiency vs. photon energy in the $\gamma\gamma 2$ apparatus as predicted by a Monte Carlo calculation. a) the photon fires at least one layer of scintillation counters; b) the photon fires at least two layers of scintillation counters.

The trigger logic requires the coincidence between the upper and lower telescopes and, for each telescope, a 6-fold coincidence among all scintillation layers; this corresponds to at least one penetrating charged particle ($T_\pi \gtrsim 120$ MeV) or to a low energy charged particle ($T_\pi \gtrsim 35$ MeV) together with one or more converted photons.

## 3. The MEA experiment

The MEA detector, the only experiment at ADONE with magnetic analysis, uses a (2 m diameter, 2 m length) solenoid mounted with its axis perpendicular to the direction of the $e^+e^-$ beams (Fig. 6)[3]. Two compensator magnets are located inside the main coil. The track curvature, due to a field of about 2.5 KG, is measured by the thin optical spark chambers $C_1$, $C_1'$ and by the wide gap cylindrical optical spark chambers $C_2$, $C_2'$.

The solid angle for magnetic analysis is $0.4 \times 4\pi$ sr. f.p.l.s. The momentum resolution is $\Delta p/p = \pm 8\%$ at $p = 1$ GeV/c.

Heavy plate optical spark chambers are placed outside the coil to identify e.m. showers, to observe interactions and to measure hadron ranges.

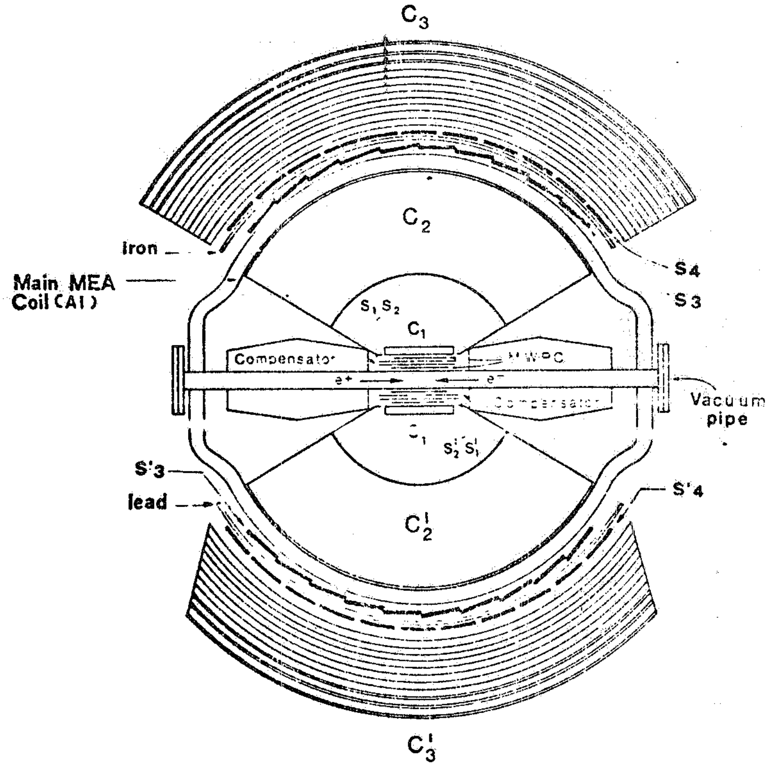


Fig. 6 The MEA experimental apparatus.

The trigger system consists of small scintillation counters $S_1 S_2$, $(S'_1 S'_2)$ just above and below the vacuum chamber, of two planes of MWPC's with wires parallel to the beams and of four hodoscopes $S_3 S_4$, $S'_3 S'_4$ outside the coil. Two particles, one in the upper part, the other in the lower part of the apparatus, are requested to trigger ($T_\pi \geq 130$ MeV).

## 4. Luminosity monitors and choice of machine operation

In addition to the small angle Bhabha scattering luminosity monitor, located in the ADONE straight section free from experiments, all three apparata detect wide angle Bhabha scattering; a double bremsstrahlung monitor is moreover associated with the $B\bar{B}$ set-up.

The MEA and $\gamma\gamma 2$ experiments use the wide angle scattering as absolute luminosity monitor. The $B\bar{B}$ experiment uses the machine luminometer as absolute monitor and checks the constancy of the luminosity thus measured against the ones measured by the double bremsstrahlung monitor and the wide angle Bhabha scattering in the apparatus.

The running of the machine for the three experiments was programmed according to decisions taken after the $J/\psi$ discovery.

A systematic search for resonances with width smaller or comparable to the machine energy spread was initiated over all of the ADONE energy domain by scanning in steps of C.M. energy $\Delta W \sim 1$ MeV and with a luminosity of 0.25 nb$^{-1}$/point. Part of these results have already been published[4].

A more careful search and more machine luminosity was invested within energy intervals where anomalies in the hadron production were

The telescopes are made of a combination of scintillation counters, optical spark chambers and lead converters arranged in such a way as to optimize the electromagnetic shower detection. The solid angle f. p. l. s. is $0.41 \times 4\pi$ sr. for triggering and $0.66 \times 4\pi$ sr. for tracking. The total thickness of the shower detector is 5.5 R. L. ; the photon detection efficiency is shown in Fig. 5 as a function of the photon energy.

The shower detector is completed by the addition of a set of eight bigap spark chambers sandwiched between nine 1.5 cm thick iron layers and covering a solid angle of $0.27 \times 4\pi$ sr. The total thickness of the apparatus corresponds to the range of a 300 MeV pion.

A pair of circular side-telescopes made of magnetostrictive spark chambers, lead absorbers and scintillation counters complete the detection system and cover an additional solid angle of $0.15 \times 4\pi$ sr.

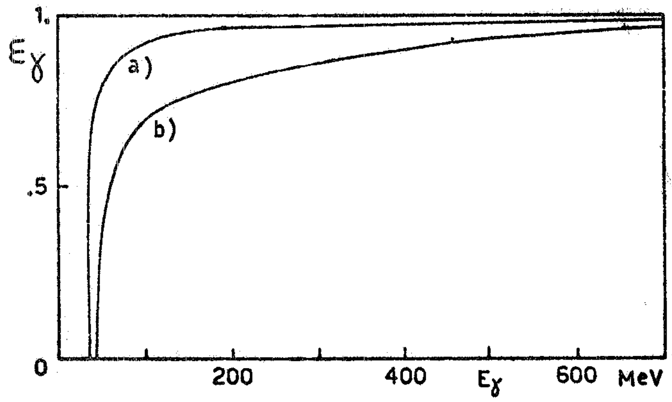


Fig. 5 Photon detection efficiency vs. photon energy in the $\gamma\gamma 2$ apparatus as predicted by a Monte Carlo calculation. a) the photon fires at least one layer of scintillation counters ; b) the photon fires at least two layers of scintillation counters.

The trigger logic requires the coincidence between the upper and lower telescopes and, for each telescope, a 6-fold coincidence among all scintillation layers ; this corresponds to at least one penetrating charged particle ($T_\pi \gtrsim 120$ MeV) or to a low energy charged particle ($T_\pi \gtrsim 35$ MeV) together with one or more converted photons.

## 3. The MEA experiment

The MEA detector, the only experiment at ADONE with magnetic analysis, uses a (2 m diameter, 2 m length) solenoid mounted with its axis perpendicular to the direction of the $e^+e^-$ beams (Fig. 6)[3]. Two compensator magnets are located inside the main coil. The track curvature, due to a field of about 2.5 KG, is measured by the thin optical spark chambers $C_1$, $C_1'$ and by the wide gap cylindrical optical spark chambers $C_2$, $C_2'$.

The solid angle for magnetic analysis is $0.4 \times 4\pi$ sr. f. p. l. s. The momentum resolution is $\Delta p/p = \pm 8\%$ at $p = 1$ GeV/c.

Heavy plate optical spark chambers are placed outside the coil to identify e. m. showers, to observe interactions and to measure hadron ranges.

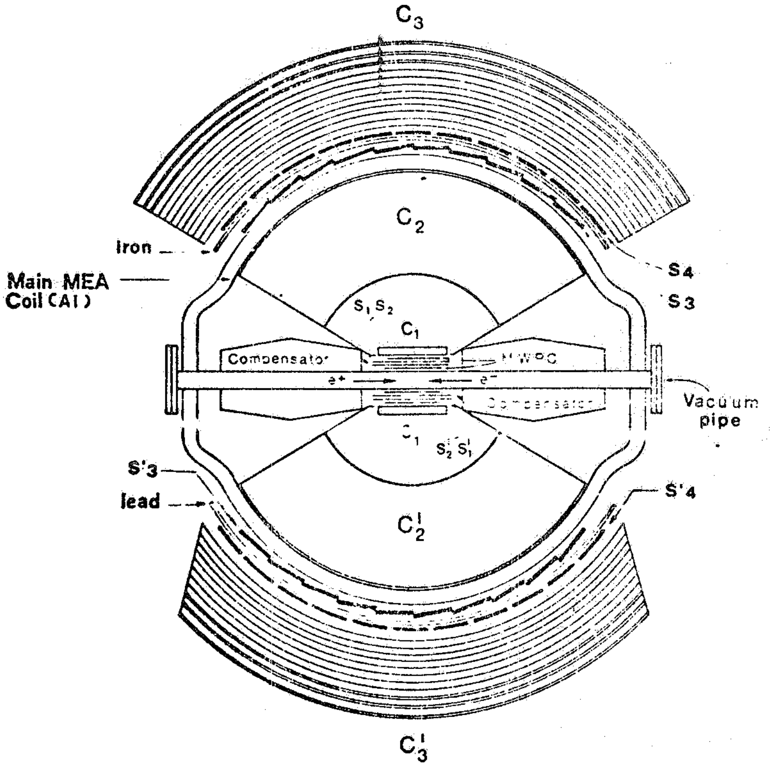


Fig. 6 The MEA experimental apparatus.

The trigger system consists of small scintillation counters $S_1 S_2$, ($S_1' S_2'$) just above and below the vacuum chamber, of two planes of MWPC's with wires parallel to the beams and of four hodoscopes $S_3 S_4$, $S_3' S_4'$ outside the coil. Two particles, one in the upper part, the other in the lower part of the apparatus, are requested to trigger ($T_\pi \gtrsim 130$ MeV).

## 4. Luminosity monitors and choice of machine operation

In addition to the small angle Bhabha scattering luminosity monitor, located in the ADONE straight section free from experiments, all three apparata detect wide angle Bhabha scattering; a double bremsstrahlung monitor is moreover associated with the $B\bar{B}$ set-up.

The MEA and $\gamma\gamma 2$ experiments use the wide angle scattering as absolute luminosity monitor. The $B\bar{B}$ experiment uses the machine luminometer as absolute monitor and checks the constancy of the luminosity thus measured against the ones measured by the double bremsstrahlung monitor and the wide angle Bhabha scattering in the apparatus.

The running of the machine for the three experiments was programmed according to decisions taken after the $J/\psi$ discovery.

A systematic search for resonances with width smaller or comparable to the machine energy spread was initiated over all of the ADONE energy domain by scanning in steps of C. M. energy $\Delta W \sim 1$ MeV and with a luminosity of 0.25 $nb^{-1}$/point. Part of these results have already been published[4].

A more careful search and more machine luminosity was invested within energy intervals where anomalies in the hadron production were suspected, typically 5 $nb^{-1}$/point in energy steps $\Delta W \sim 5$ MeV.

## III RESONANT PRODUCTION OF $K^*$ AT W = 2.13 GeV

The systematic scanning by the MEA group showed an anomalous behaviour of the multihadron yield in the energy interval $2070 < W < 2200$ MeV.

The analysis concentrated on events with at least three charged particles detected ($\gtrsim 3$ C); background contamination in this category was found to be neglegible. Preliminary data have already been reported[5].

To better explore the detected effects, new data were collected at the three fixed energies W = 2.13, 2.25, 2.30 GeV. 87 events, corresponding to a luminosity of 47 $nb^{-1}$, were put together by the first energy scanning; 90 events, corresponding to a luminosity of 37.5 $nb^{-1}$, were recently obtained at the three fixed energies.

During this last data taking a counter system to measure time of flight (TOF) went into operation; the combined measurement of momentum and TOF gave then informations on the nature of particles reaching the TOF counters. Some extra information for particle identification could also be obtained by nuclear interaction or decay of hadrons reaching the range chambers outside the magnet coil.

### 1. Effective mass spectra

The effective mass spectra of two particle neutral systems were constructed for all hadronic events; each track in a neutral pair was alternatively assumed to be a $\pi$ or a K giving rise therefore to three possible combinations $(\pi\pi)^o$, $(\pi K)^o$, $(K\bar{K})^o$.

A statistical weight was attributed to each pair so that the total event weight added up to one, whatever the number of tracks in the event. The information on the particle nature from TOF or range chambers was used, if available, in the form of a definite probability for being a $\pi$ or a K attached to the particle.

The mass distributions for $(\pi\pi)$ or $(\pi K)$ combinations are presented in Fig. 7. The upper part of the figure corresponds to C.M. energies W between 2120 and 2140 MeV, the lower part to energies outside this interval. Some evidence for $K^*$ production is visible in the $(\pi K)$ distribution of Fig. 7a; some evidence for $\rho$ production is visible in the $(\pi\pi)$ distribution of Fig. 7b.

The mass resolution of the MEA magnetic detector is $\sigma_M \sim 50$ MeV/$c^2$ at M $\sim$ 890 MeV/$c^2$.

The dashed area of Fig. 7a shows the effect of kinematical reflections, i.e. events which, if assumed to be $(\pi K)$ combinations fall in the $800 < M_k < 1000$ MeV/$c^2$ mass band. Similarly the dashed area of Fig. 7b corresponds to events which, if assumed to be $(\pi\pi)$ combinations, fall in the $\rho$ mass band. Kinematical reflections therefore do not explain the $K^*$

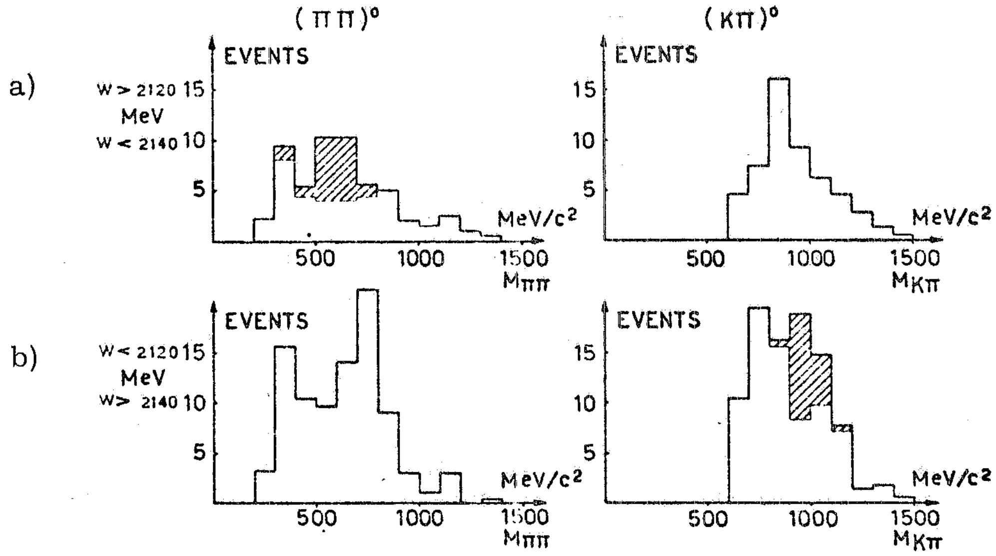


Fig. 7 Effective mass distribution for $(\pi\pi)^o$ and $(\pi K)^o$ combinations out of multiparticle hadronic events. a) $2120 < W < 2140$ MeV (in resonance region); b) $W < 2120$ $W > 2140$ MeV (outside resonance region). Dashed areas indicate the effect of $\rho$ and $K^*$ kinematical reflections.

enhancement in Fig. 7a. Further on, to reduce the effects of kinematical reflections, slightly asymmetric cuts in the $M(\pi K)$ mass were applied to extract the $K^*$ yield from all hadronic events ($800 < M_{\pi K} < 950$ MeV/c$^2$).

$K^*$ production is more clearly visible in the effective mass spectrum of the particle combinations for which a $K/\pi$ discrimination by momentum and TOF is available. The $K^*$ signal is present at W = 2130 MeV and absent at energies 2250 and 2300 MeV (Fig. 8).

The final state of three hadronic events could be fully reconstructed and it came out to correspond to $K^*\bar{K}^*$ production.

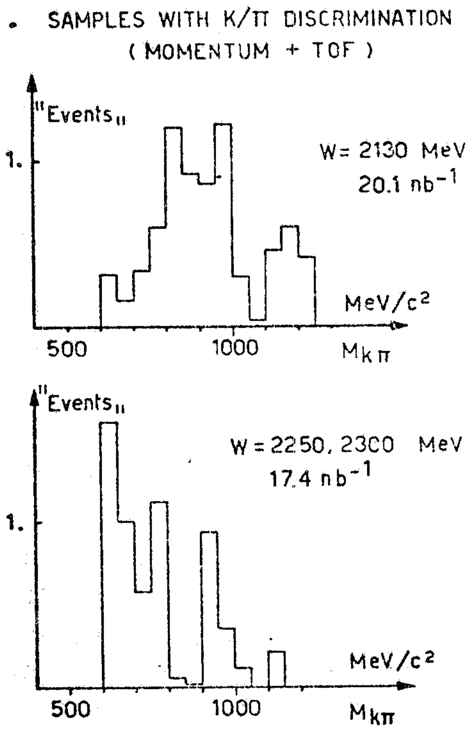


Fig. 8 $(\pi K)^o$ effective mass distributions for sample with $K/\pi$ discrimination.
a) W = 2130 MeV, at the resonance;
b) W = 2250, 2300 MeV, far from the resonance.

## 2. $K^*$ production

The yield for $K^*$ production as a function of the C. M. energy W is presented in Fig. 9 ; one can notice a very clear resonant behaviour, centered at W = 2.130 GeV and with width $\Gamma$ of about 30 MeV.

If the non resonant background is interpolated by a straight line, the expected number of events in the region $2.0 < W < 2.14$ GeV is $12.5 \mp 1.2$ eV ; the observed events are $28.1 \pm 2.6$ ev with an enhancement of $15.6 \pm 2.9$ ev corresponding to a statistical significance for the effect of more than 5 standard deviations[6].

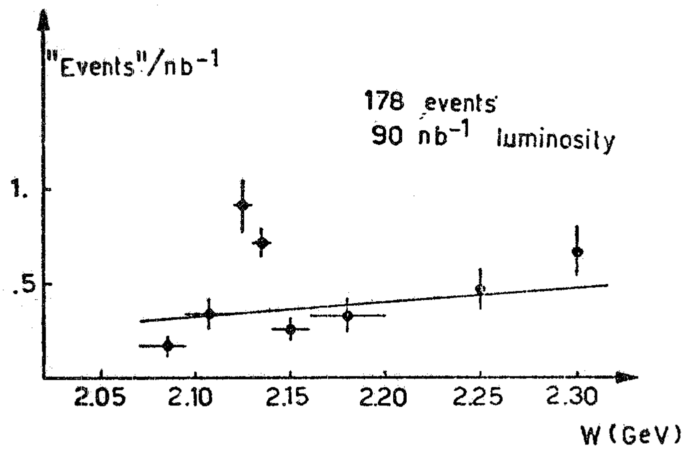


Fig. 9 $(\pi K)^o$ yield vs. C. M. energy W. ( $800 < M_{\pi K} < 950$ MeV/$c^2$ ).

## 3. Nature of the 2130 MeV/ $c^2$ resonance

The narrow width and the large $K^*$ production, through which the resonance was identified, is suggestive of a recurrence of the $\varphi$(1020) meson. Radial excitation of the $\varphi$ meson and a $\lambda\bar{\lambda}$ quark spectroscopy are expected in the energy region explored by ADONE[7,8]. Their positions, predicted by a Veneziano mass formula of the type :

$$M_n^2 = M_\varphi^2 + n(\approx 2 M_\rho^2) \qquad n = 1, 2, .. \qquad (1)$$

are 1490, 1840, 2140 MeV/ $c^2$.

The resonance at 2130 MeV is then a possible candidate for the $\varphi'''$ recurrence. It is worth noting though, that while the $K^*$ production is enhanced at W = 2130 MeV, simple K production is rather surprisingly constant within statistics (K/TOT : $(8.2 \pm 3.3)\%$ at W = 2130 MeV ; $(10.5 \pm \pm 4.3)\%$ at W = 2300 MeV).

If the scheme relative to $\varphi$ excitations is correct, other narrow structures might appear around W equal to 1.8 and 1.5 GeV. This observation determined the subsequent use of ADONE luminosity which was therefore alternatively shared between the two mentioned energy regions.

## IV THE 1.8 GeV ENERGY REGION[9]

The first indication of the presence of a structure in the yield for the reaction $e^+e^- \rightarrow$ hadrons, was obtained during an energy scanning in the autumn 1976. Much more luminosity was used at prefixed energies in two other long periods of running from February to March and from April to May 1977.

The data, relative to hadronic events with at least three charged particles (≥ 3C), by the MEA group (300 events, L = 123 $nb^{-1}$) are presented in Fig. 10. Only statistical errors are quoted; the experimental points, measured in different running periods, are in good overall agreement and are plotted in Fig. 10 by different symbols.

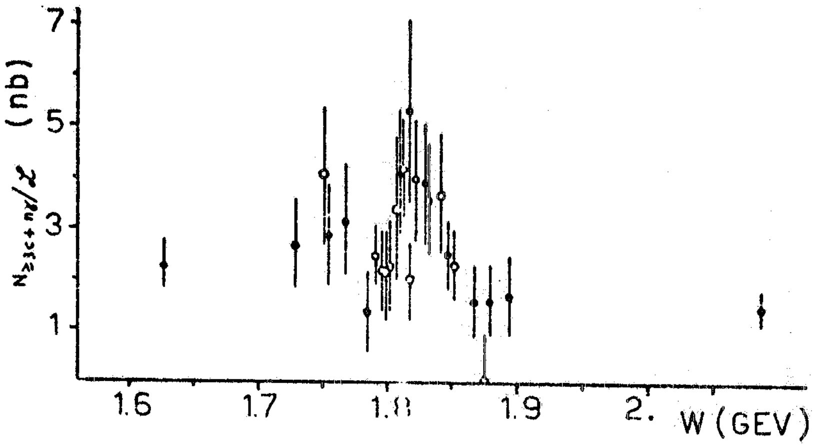


Fig. 10 Yield vs. W for (≥ 3C) hadronic events as measured by the MEA group. Data collected in different running periods are plotted by different symbols: o September-October 1976 (energy scanning); ● February-April 1977 (prefixed energies).

Since the $B\bar{B}$ data (700 events, L = 70 $nb^{-1}$) were collected at prefixed values of the machine energy, while part of the MEA data were collected by energy scanning, the experimental results of the two groups are compared in Fig. 11 after grouping MEA data close in energy.

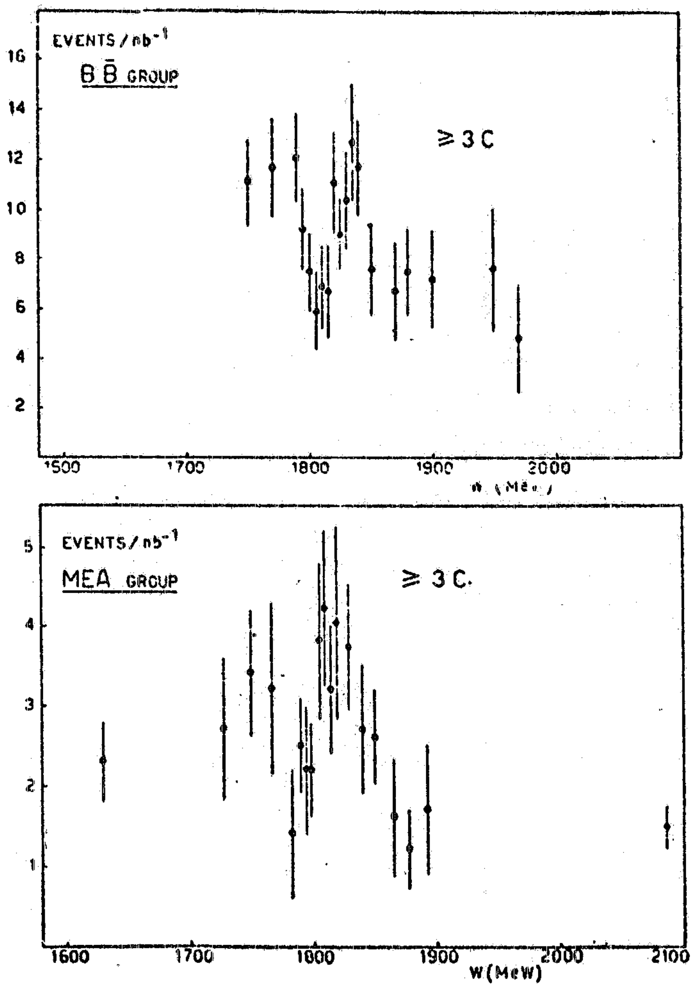


Fig. 11 Comparison of the yields vs. W for (≥ 3C) hadronic events as measured by the $B\bar{B}$ and MEA groups.

The overall aspect of the hadronic yields is very similar although, as it was already pointed out, the angular coverage and the trigger energy cuts of the two experiments are quite dissimilar. It is possible to notice however a shift of about 15 MeV towards higher energies of the data pattern observed by the $B\bar{B}$ group compared to the one observed by the MEA group.

The fast twist of the hadronic yield seen by the two experiments is suggestive of a dispersive contribution and of an interference between two nearby resonances. Evidence for a rather wide resonance at about W = = 1780 MeV, interpreted as an $\omega'$ (so with negative G-parity), was indeed recently published by an Orsay group[10].

The $B\bar{B}$ yield for ($\geq$ 3C) hadronic events is compared in Fig. 12 with the Orsay results in the same channel; only statistical errors are quoted. The comparison is particularly significant since both apparata have cylindrical symmetry around the $e^+e^-$ beams and cover a similar solid angle. An arbitrary scale factor between the two sets of data is applied in Fig. 11 to take into account the difference in overall detection efficiency of the two apparata[11]. Although the energy spacing of the Orsay experimental points is rather large, there is a fair agreement with the $B\bar{B}$ data at the high yield around 1770 MeV at the low yield around 1800 MeV and on the right of the sharp structure observed at ADONE.

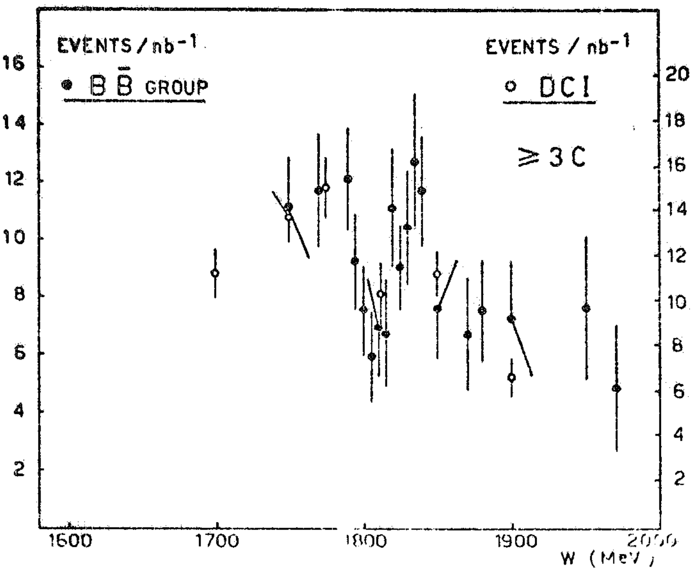


Fig. 12 Comparison of the yields vs. W for ($\geq$ 3C) hadronic events as measured by the $B\bar{B}$ ADONE group (•) and by the DCI group (o).

The statistical significance of the structure seen by the three ADONE experiments was studied in various ways. Tests applied to the $B\bar{B}$ data produced the following results. The distribution of the experimental points around a fitted constant value of 8.7 eV/nb$^{-1}$ gives a $\chi^2$/d.f. = 27/18 corresponding to a confidence level of 0.09.

The true confidence level is indeed much lower then this limit, since the correlation among the points carries additional information. The "one sample runs test"[12], deviced to probe the randomness of the data around the average value of 8.7 eV/nb$^{-1}$, gives a confidence level below 0.025 for the occurence of a fluctuation similar to that seen in the data; therefore both the dispersion and the correlation of the experimental points make it very unlikely that the effect at 1.8 GeV is due to chance. From the comparison of the average event rate at the five energies between 1820 and 1840 MeV (PEAK) and the other ten energies (BACKGROUND) one gets :

$$\text{PEAK} = 10.4 \pm 0.8 \ \text{ev/nb}^{-1}, \qquad \text{SIGNAL} = 3.6 \pm 1.0 \ \text{ev/nb}^{-1}$$

$$\text{BACKGROUND} \quad 6.8 \pm 0.6 \ \text{ev/nb}^{-1} .$$

The existence of a new structure in the explored energy region is demonstrated within 3.6/1 standard deviations, corresponding to a confidence level of $4 \times 10^{-4}$ for an accidental result.

Similar analyses, performed on the data obtained by the MEA and $\gamma\gamma 2$ groups, gave equivalent results. The fact that the three largely independent ADONE experiments observed similar effects gives additional confidence on the existence of a bona fide resonance in the 1.8 GeV energy region.

## 1. Nature of the 1820 MeV resonance

Some insight on the nature of the 1820 MeV resonance comes from the data collected by the $\gamma\gamma 2$ group. This experiment has a very good efficiency for $\gamma$ detection (see Fig. 5); it is then possible to separate hadronic channels where $\gamma$'s are or are not present.

The data in the peak region, corresponding to a total luminosity of 65 $nb^{-1}$, are shown separately (see Fig13) for hadronic events with three or four charged particles plus at least one gamma ray detected ($3,4\ C + \geq 1\gamma$; 119 events), and for three or four charged particles without detected gammas (3,4 C; 186 events). While the 1.8 GeV structure clearly appears in the first category (Fig. 13a), it seems to be absent in the second one (Fig. 13b). This would suggest a dominant channel $2\pi^+ 2\pi^- \pi^0$. The $2\pi^+ 2\pi^- 2\pi^0$ channel, which is also a possible candidate, should be accompanied by the same G-parity channel $2\pi^+ 2\pi^-$; this seems to be excluded by the data.

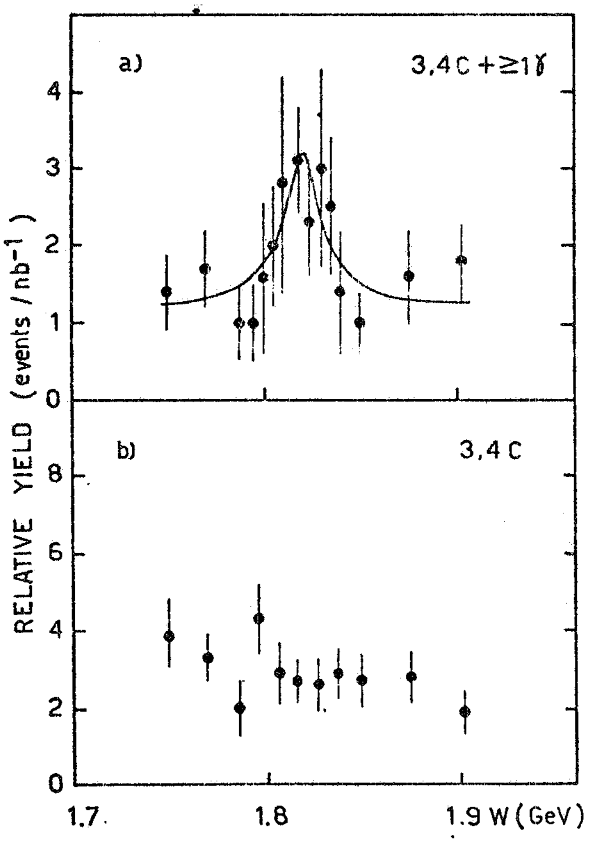


Fig. 13 Yields vs. W for :
a) ($3,4\ C + \geq 1\gamma$) hadronic events;
b) (3,4 C) hadronic events
as measured by the $\gamma\gamma 2$ group.

What has been said gives indications for a negative G-parity of the 1820 MeV resonance, a necessary condition for a possible interference with a nearby $\omega'$ resonance.

One might notice at this point that the energy position of the new ADONE structure fits rather well the expectations for the mass of the second radial excitation $\varphi''$ of the $\varphi$, predicted by the Veneziano mass formula (1).

Were the 1.8 GeV truly a $\varphi$ recurrence one would expect OZI[13] rule allowed decays to dominate i. e.

$$\begin{aligned} \Phi'' &\longrightarrow \varphi\pi\pi \\ &\longrightarrow \varphi'\pi\pi \\ &\longrightarrow K^*\bar{K},\ K\bar{K}^* \\ &\longrightarrow K^*\bar{K}^* \quad \text{etc.} \end{aligned}$$

The detection efficiency of the $\gamma\gamma 2$ exp. for all these channels satisfy the inequality $\varepsilon(3,4\,C + \geq 1\gamma) < \varepsilon(3,4\,C)$; they do not probably dominate since, as already observed, the 1.8 GeV resonance clearly appears only in the $(3,4\,C + + \geq 1\gamma)$ and not in the (3, 4 C) hadronic yield.

The observation of a copius K production at $W \sim 1.82$ GeV would be a good signature for a $\varphi$ recurrence. The MEA group, which is the most properly equipped for $K/\pi$ discrimination by momentum + TOF determination, is presently performing the accurate film measurements needed for identifying K's ; a quantitative answer on the K production yield will be available only in a few months time.

A search for K's is also possible with the $B\bar{B}$ apparatus (mass separation for low energy K's by the "dE/dx vs. E method", or by observation of K's decays) and with the $\gamma\gamma 2$ apparatus (range and K decays) ; this investigation is under way. The only conclusion possible now on the $K/\pi$ ratio is that all the three experiments have no indications for a strong K production yield in the 1.8 GeV region.

Note also that, at these low energies, the detection efficiency of the apparata, changes considerably if the final states contain massive particles like K's in addition to $\pi$'s ; it will be difficult to extract reliable cross section measurements from experimental data until the decay channels of the 1.8 GeV resonance are more clearly identified.

## 2. Fits to the 1.8 GeV data

Fits to the data presented by each group were independently attempted; some of the results can be found in Table II.

The $B\bar{B}$ group used the following ingredients : a straight line background, two Breit-Wigner ($BW_1$, $BW_2$, of masses $M_1$ and $M_2$), the interference between two of the three listed contributions ; in fit 1 of Table II the two BW interfere, in fit 2 no interference is present.

TABLE II

Mass and width of the $BW_2$ resonance as obtained by best fitting the data of the three experiments. In parentheses are reported the values obtained by the $B\bar{B}$ group for the Breit-Wigner in the 1750 - 1800 MeV region ($BW_1$).

| | | MASS (MeV) $M_2$ $M_1$ | WIDTH (MeV) $\Gamma_2$ $\Gamma_1$ | $\chi^2$/d.f. |
|---|---|---|---|---|
| (1) | $B\bar{B}$ with interference | $1812^{+7}_{-13}$ $(1792^{+31}_{-14})$ | $34^{+21}_{-15}$ $(79^{+77}_{-29})$ | 6.1/9 |
| (2) | $B\bar{B}$, without interference | $1836^{+3}_{-3}$ $(1765^{+14}_{-38})$ | $13^{+3}_{-2}$ $(47^{+25}_{-20})$ | 8.8/11 |
| (3) | $\gamma\gamma 2$ | $1819 \pm 5$ | $24 \pm 5$ | 6.6/11 |
| (4) | MEA | $1821 \pm 16$ | $31 \pm 15$ | 10/14 |

One can notice that :

a) The fitted position of $M_2$ is very dependent on the presence of the interference term. The fitted $M_2$ value can be somewhat different from the mass position of the peak seen in the data. The interpretation of this fact is related to the two parts into which a BW can be decomposed : a "dispersive" term and an "absorbitive" one (see Fig. 14); the relative

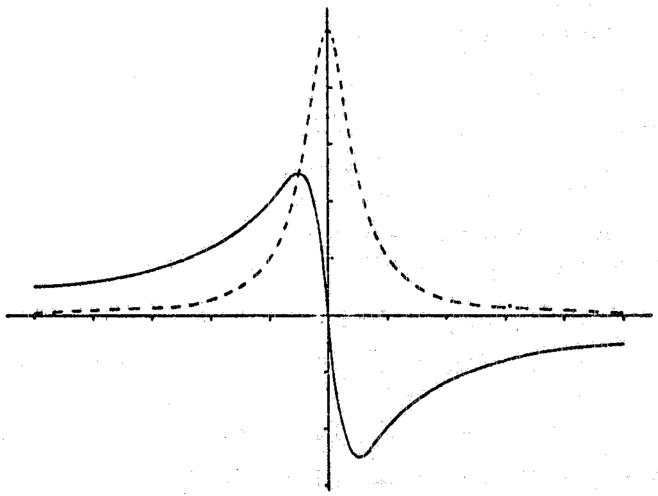

$$f(W) = A(W)e^{i\Phi} + \frac{A_1 M_1^2 e^{i\Phi_1}}{M_1^2 - W^2 - i M_1 \Gamma_1} + \frac{A_2 M_2^2 e^{i\Phi_2}}{M_2^2 - W^2 - i M_2 \Gamma_2}$$

Fig. 14 Decomposition of a BW into "dispersive" (———) and "absorbitive" (- - - -) parts. The parts from $BW_1$ and $BW_2$ play roles determined by the parameters $A$, $A_1$, $A_2$, $\Phi$, $\Phi_1$, $\Phi_2$, $M_1$, $M_2$, $\Gamma_1$, $\Gamma_2$.

influence of the two terms, and a consequent apparent energy shift of the resonance in the data depends on the amplitudes A, $A_1$, $A_2$, on the resonance widths $\Gamma_1$ and $\Gamma_2$ and on the relative phases $\Phi$, $\Phi_1$, $\Phi_2$[14].

b) The fit admits the presence of an $\omega'$ resonance[10], but due to the sharp decrease of the yield at energies higher than the $\omega'$ peak, it prefers a smaller width than the one indicated by the Orsay group[15].

c) Although the introduction of the interference term slightly improves the fit, the question about the existence of the interference term cannot be settled at the present stage.

In Fig. 15 the $B\bar{B}$ fits are superimposed to the $B\bar{B}$ data; in addition to fits 1 and 2 of Table II, Fig. 15 shows also a third fit where a linear background, two BW's and the interference between the $BW_2$ and the background is considered.

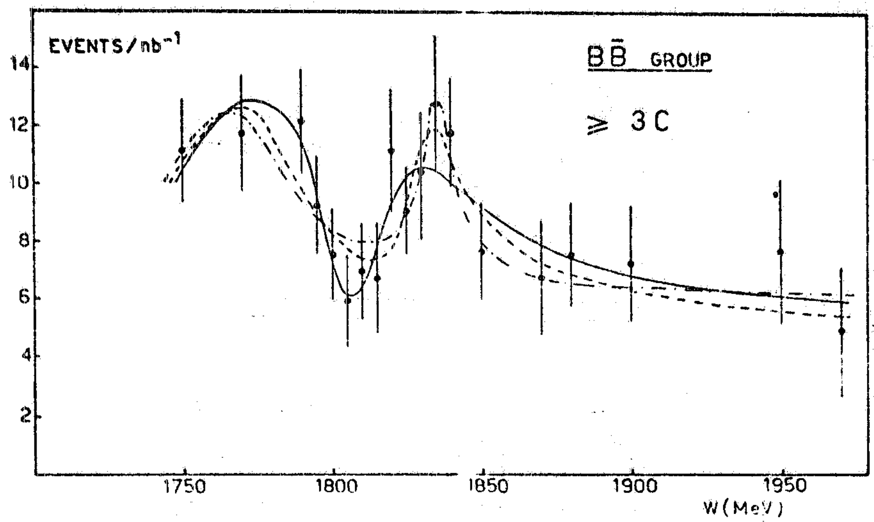


Fig. 15 Fits to the $B\bar{B}$ yield vs. W for ($\gtrsim$3C) hadronic events.
Fit 1 Table II —— (linear term + $BW_1$ + $BW_2$ + interference ($BW_1$, $BW_2$))
Fit 2 Table II ---- (linear term + $BW_1$ + $BW_2$)
—·— (linear term + $BW_1$ + $BW_2$ + interference ($BW_2$, linear term)).

Quite acceptable interpolations (3 and 4 in Table II) of the MEA and $\gamma\gamma 2$ data are possible by using a linear background and a single BW. Since a reasonable agreement is present among the fits 1, 3, 4, relative to the three ADONE experiments, an overall general fit to the ($\gtrsim$3C) yields of the $B\bar{B}$, $\gamma\gamma 2$ and MEA experiments was attempted. The parameters $M_1$, $\Gamma_1$, $M_2$, $\Gamma_2$ were kept fixed and with values $M_1$ = 1778 MeV, $\Gamma_1$ = 75 MeV, $M_2$ = = 1812 MeV, $\Gamma_2$ = 37 MeV; the amplitude of the linear background, of the two BW's and the phase of the interference term between the two BW's were instead left free. The resulting fit is quite satisfactory and it is presented in Fig. 16; maximum negative interference is demanded by the three sets of data.

Note that the different energy position of the 1.8 GeV peaks in the $B\bar{B}$ on one side and the MEA and $\gamma\gamma 2$ experiments on the other side, is nicely accommodated and it is related to the role of the interference term.

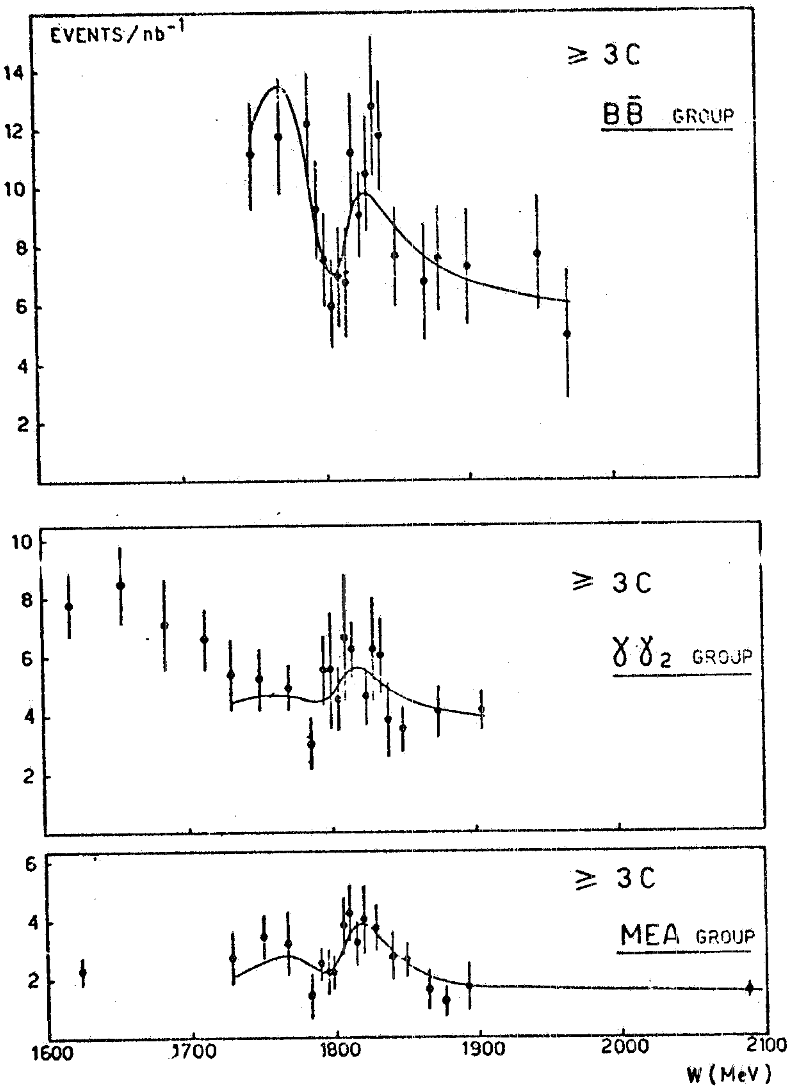


Fig. 16 General fit to the yield vs. W for the (≳3C) hadronic events of the B$\bar{B}$, γγ2, MEA experiments. (Linear term + $BW_1$ + $BW_2$ + interference ($BW_1$, $BW_2$)). Resonance masses and widths are fixed. Amplitudes of the linear term, of $BW_1$, of $BW_2$ and the interference phase were left free.

## V THE 1.5 GeV REGION

Following the suggestion by the mass formula (1), the 1.5 GeV energy region was explored almost contemporarily and in alternance with the 1.8 GeV region. The experimental results I shall present should be considered preliminary, since the analysis is not fully completed; moreover, the data taking in this energy domain will go on for several extra months.

A first part of the data, corresponding to 500 (≳2C) hadronic events and to a luminosity of 19 nb$^{-1}$ for the B$\bar{B}$ group, and to 430 events (≳2C) and 28 nb$^{-1}$ for the γγ2 group was analysed between the energy limits 1470 and 1570 MeV.

The yields for events with at least two charged particles (Fig. 17) shows a clear narrow signal at an energy W of about 1500 MeV[16]. If a constant background is fitted to all the experimental points, the signal (the 5 highest points for the $B\bar{B}$ experiment, the 3 highest points for the $\gamma\gamma 2$ experiment) has a statistical significance of the order of 3.5 - 4.0 standard deviations for each of the two experiments.

A Breit and Wigner + constant term fit suggests a width certainly less than 4 MeV for the structure.

If radiative corrections[17] (~17% of the integrated yield) and the energy resolution of the machine are taken into account, the fitted widths $\Gamma$ are of the order of 2.5 MeV ($M = 1499^{+0.5}_{-0.7}$, $\Gamma = 2.3^{+0.5}_{-0.3}$ for the $B\bar{B}$ experiment). This value is an indication for a very narrow resonance, but it must be taken with care since the rather complex structure of the hadronic yield in this energy domain might demand a more refined analysis later on.

While the mass of the resonance is in good agreement with what predicted by the mass formula for the first $\varphi$ recurrence, $\varphi'$, the width of the new structure is much smaller than the predicted value, which ranges from 25 to 50 MeV for such a state[7,8].

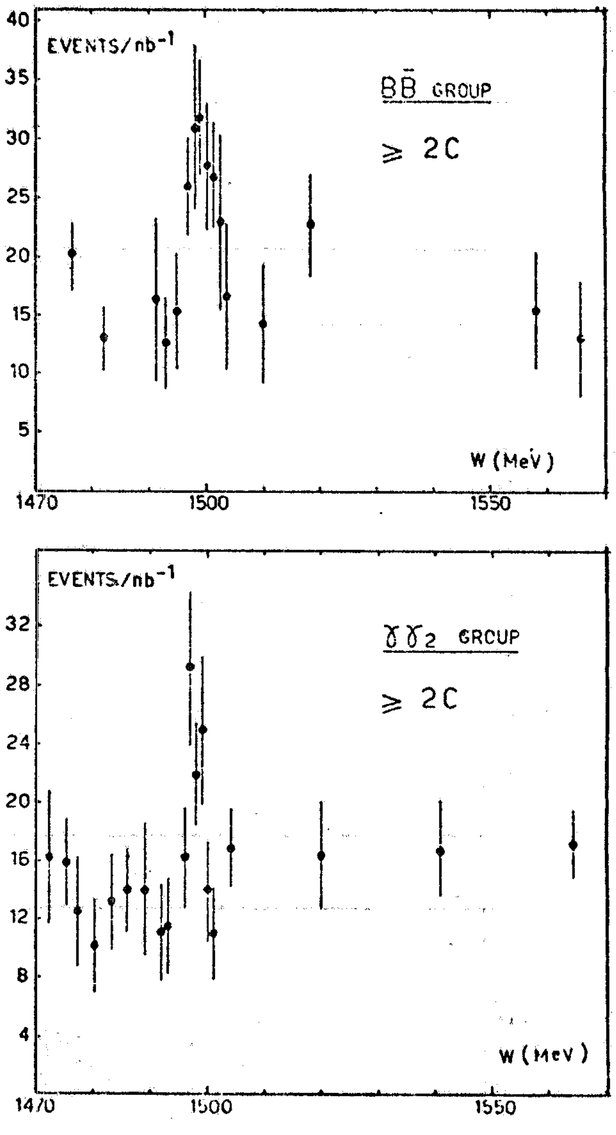


Fig. 17 Yield vs. W for (≥2C) hadronic events as measured by the $B\bar{B}$ and $\gamma\gamma 2$ groups around 1.5 GeV.

Greco[18] suggested then that the 1.5 resonance might be identified with a $^3D_1$ ($\lambda\bar{\lambda}$) state; were this the right interpretation, a $^3S_1$ ($\lambda\bar{\lambda}$) state should be located close and at lower energies. The width of the $^3S_1$ state would be larger than the one of the $^3D_1$ state although not as large as 25 MeV since this lower energy resonance would be closer to the $K\bar{K}^*$ threshold. Interference effects between the S and D states would also be possible. These predictions on $\lambda\lambda$ quark spectroscopy, if correct, would reproduce the situation of $c\bar{c}$ spectroscopy with its $\psi'$ $^3S_1$ level and the $^3D_1$ (3.78 GeV) recently discovered narrow state[19].

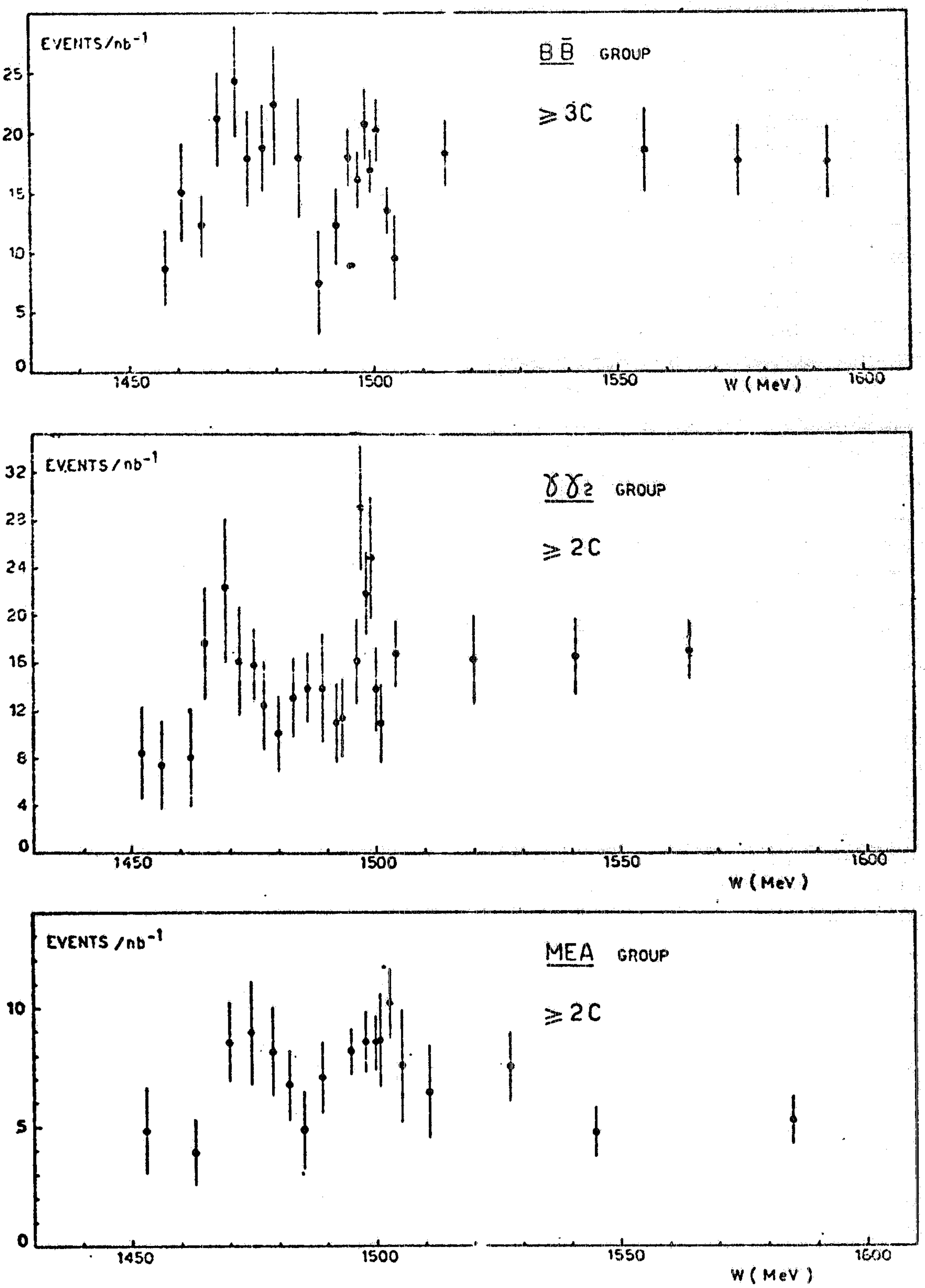


Fig. 18 Yield vs. W for ($\gtrsim$3C) hadronic events ($B\overline{B}$ group); Yield vs. W for ($\gtrsim$2C) hadronic events ( $\gamma\gamma 2$ and MEA groups). A recent low luminosity exploration of the energy region 1450 < W < 1490 MeV.

A low luminosity exploration of the energy region between 1450 and 1490 MeV and some extra luminosity taken between 1490 and 1560 MeV give indeed an indication of the presence of another structure. The measured yields of the three experiments are shown together in Fig. 18 ; they correspond to a luminosity of 39 $nb^{-1}$ for the $B\bar{B}$ experiment, 35.4 $nb^{-1}$ for the $\gamma\gamma 2$ experiment, and 57 $nb^{-1}$ for the MEA experiment.

The data are the one relative to the (≥2C) hadronic events for the MEA and $\gamma\gamma 2$ experiments and to (≥3C) hadronic events for the $B\bar{B}$ experiment, since,due to the lower energy cuts of this last experiment, the rejection of cosmic rays and machine generated background requires a careful analysis of the (2C) channel which has not been completed yet.

The total number of hadronic events is at present 673 (≥3C) for the $B\bar{B}$ group, 544 (≥2C) for the $\gamma\gamma 2$ group and 434 (≥ 2C) for the MEA group. The yield for events with 4 charged particles (4C) seen in the $B\bar{B}$ apparatus is also shown in Fig. 19.

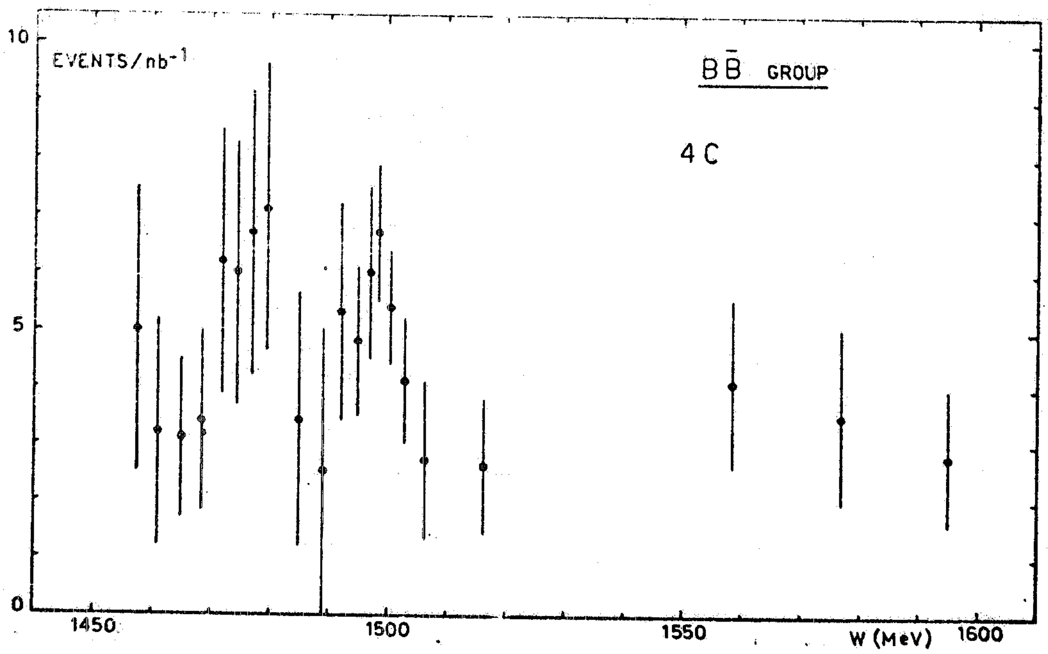


Fig. 19 Yield vs. W for (4C) hadronic events as measured by the $B\bar{B}$ group.

From the data of the three experiments a rather complex situation emerges for the hadronic yield in the 1.4-1.6 GeV energy region; this demands for a more complete exploration and for a larger investment of machine luminosity.

## 1. Nature of the 1.5 GeV state

As in the case of the 1.8 GeV structure, a clear identification of the 1.5 state as a $(\lambda\bar{\lambda})$ quark compound would be the indication of copious decays via strange meson channels like $\varphi\pi\pi$, $K\bar{K}^*$, $K\bar{K}$, etc.

A search for K's by the methods previously described just started. Branching ratios to detectable final states, geometry and energy cuts, and in general all requirements needed to identify "K states" at these low C. M. energies make the detection efficiency very small (typically 0.5% for a $K\bar{K}^*$ state in the $\gamma\gamma 2$ apparatus). The three experiments can only state that no evidence is available yet for copious decays via "K" channels.

An interesting study to clarify the nature of the 1.5 GeV resonance was made by the $\gamma\gamma 2$ group. Their apparatus has a good detection efficiency for both charged particles and $\gamma$ rays. They tried to solve the system of equations $N_k = \varepsilon_{ki}\sigma_i$, where $N_k$ is the number of events in a certain category k (i.e. (2C), (2C+$\gamma$), (3C), etc.), $\sigma_i$ are the cross sections for the production of neutral and charged pions with multiplicity i, $\varepsilon_{ki}$ is the efficiency for detecting the $\sigma_i$ cross section in the k-category. The elements of the $\varepsilon_{ki}$ matrix were calculated by assuming final states with only pions present and distributions according to an invariant phase space.

Due to the rather low statistics the results must be considered preliminary; they are presented in Fig. 20. The cross sections (in arbitrary

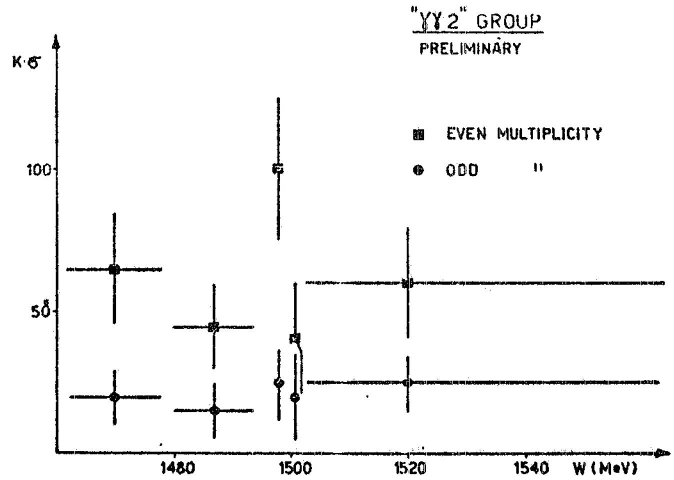


Fig. 20 Preliminary results on the decomposition of the hadronic cross section into a part with positive G-parity (even number of pions produced) and a part with negative G-parity (odd number of pions produced). At the new resonance positive G-parity is preferred.

units) for states with an odd $\sigma_0$ and with an even number of pions $\sigma_E$ are plotted separately. A large increase of the sole $\sigma_E$ cross section seems to take place in passing through the 1.5 GeV structure. This would suggest a positive G-parity, opposite to what one would expect for a $\varphi$ recurrence.

## 2. Barionium ?

The narrow width of the 1.5 GeV state, the indication for positive G-parity, the lack of abundant decays to strange particles, advice to be cautious before identifying the new resonance with a $(\lambda\bar{\lambda})$ quark state, even if its mass is in agreement with the predictions of the Veneziano mass formula (1).

A possibility one should consider is that in the ADONE energy domain and close to the threshold for the reaction $e^+e^- \rightarrow p\bar{p}$, barionium states might be present and might contribute to the $e^+e^-$ annihilation into hadrons. Barionium states have since long been predicted by the one boson exchange potential model (OBEP)[20] and by duality requirements and quark models[21]. These states should be preferentially coupled to decay channels involving barions if $M > 2\, m_p$; if $M < 2\, m_p$ they can only decay to mesons although something similar to the OIZ rule (related to barion number and not to strangeness or charm) would forbid these decays. Due to this last observation, the widths of barionium states at masses lower or close to $2\, m_p$ are expected to be very narrow with $\Gamma$'s even of the order of a few MeV.

Regge trajectories[21, 22] and radial excitations of barionium states might also be foreseen; no prediction is available at present for a possible coupling of these states to the $e^+e^-$ annihilation channel.

Experimental evidence in favour of barionium states has been accumulating during last months for $M > 2\, m_p$[23]. More recently, indications for bound states with $M < 2\, m_p$ have been obtained[24].

## CONCLUSIONS

The region between 1.4 and 2.5 GeV seems to present to an experimental investigation a much greater complexity than expected. In this energy region recurrences of known vector mesons were foreseen. Exotic possibilities, like barionium states, must now also be considered. A more refined scanning of the region of interest, larger statistics, the study of exclusive decay channels, are needed before that the nature of the new ADONE resonances might be fully recognized.

The outlined program is slowly carried on. The sense of surprise we feel in front of the new resonances and the questions they rise are meanwhile well symbolized in Fig. 21[25].

Fig. 21 Open questions about the nature of the new resonances.

## NOTES AND REFERENCES.

(1) The authors who contributed to the material presented in this talk are:

| FRASCATI-NAPLES PISA-ROME | FRASCATI-ROME | FRASCATI-MARYLAND NAPLES-PADUA-ROME |
|---|---|---|
| B $\bar{B}$ | $\gamma\gamma 2$ | MEA |
| M. AMBROSIO<br>G. BARBARINO<br>G. BARBIELLINI<br>A. BARLETTA<br>C. BEMPORAD<br>R. BIANCASTELLI<br>G. BROSCO<br>M. CALVETTI<br>M. CASTELLANO<br>F. COSTANTINI<br>G. GIANNINI<br>P. LARICCIA<br>G. PATERNOSTER<br>S. PATRICELLI<br>L. TORTORA<br>U. TROYA | C. BACCI<br>R. BALDINI CELIO<br>G. CAPON<br>R. DEL FABBRO<br>G. DE ZORZI<br>E. IAROCCI<br>G. P. MURTAS<br>G. PENSO<br>M. SPINETTI<br>B. STELLA | R. BERNABEI<br>S. D'ANGELO<br>B. ESPOSITO<br>F. FELICETTI<br>A. MARINI<br>P. MONACELLI<br>M. MORICCA<br>A. NIGRO<br>L. PAOLUZI<br>P. PATTERI<br>L. PESCARA<br>G. PIANO MORTARI<br>P. ROSINI<br>F. RONGA<br>A. SCIUBBA<br>A. SEBASTIANI<br>B. SECHI-ZORN<br>F. VANOLI<br>G. T. ZORN |

(2) J. D. Bjorken, in "Proceedings of the 1975 Intern. Symp. on Lepton and Photon Interactions at High Energy", Stanford, 1975.
(3) W. W. Ash et al., Frascati report LNF-77/18 (1977).
(4) R. Baldini-Celio et al., Phys. Letters 58B, (1975) 481;
C. Bacci et al., Phys. Letters 64B, (1976) 356;
B. Esposito et al., Phys. Letters 58B, (1975) 478;
B. Esposito et al., Phys. Letters 64B, (1976) 362;
G. Barbiellini et al., Phys. Letters 64B, (1976) 359.
(5) R. Barnabei et al., Frascati report LNF-76/64 (1976).
(6) An additional evidence for the presence of a resonance at $M \sim 2130$ MeV/$c^2$ in the $K\pi K\pi$ effective mass spectrum, comes from the Cornell LAME exp. The data were presented by L. Hand at this Symposium.
(7) M.Greco, Frascati report LNF-76/55 (1976).
(8) F. M. Renard, Nuclear Phys. B82, (1974) 1.
(9) Part of the results have already been published in the articles:
B. Esposito et al., Phys. Letters 68B, (1977) 389;
C. Bacci et al., Phys. Letters 68B, (1977) 393;
G. Barbiellini et al., Phys. Letters 68B, (1977) 397.
(10) G. Cosmé et al., Phys. Letters 67B, (1977) 231.

(11) The detection efficiency of the $B\bar{B}$ exp. for a $4\pi^{\pm}$ state generated according to an invariant phase space is of the order of 30%.
(12) A. Swed et al., Annals of Math. Statistics 14, (1943) 83.
(13) S. Okubo, Phys. Letters 5, (1963) 165;
G. Zweig, CERN Report $\bar{S}$ 419/TH 412 (1964);
J. Iizuka et al., Prog. Theor. Phys. 35, (1966) 1061.
(14) A very similar situation is the one of $\rho$-$\omega$ interference in $e^+e^-$ reactions. See D. Benaksas et al., Phys. Letters 39B, (1972) 289.
(15) New Orsay data, supporting this indication were presented by F. Laplanche at this Symposium.
(16) The relevant decay channels of the new 1.5 GeV are not known yet; this limits the evaluation of detection efficiencies and of the integrated cross section for its production. Under the hypothesis of only decays into pions, distributed according to an invariant phase space, the integrated cross section for the production of the new state is of the order of 700 nb·MeV. The coupling to the photon is certainly $\Gamma_e < 100$ eV.
(17) M. Greco et al., Nuclear Phys. 101B, (1975) 234;
J. D. Jackson, Nuclear Instr. and Meth. 128, (1975) 13.
(18) M. Greco, Frascati report LNF-77/30 (1977).
(19) P. A. Rapidis et al., Phys. Rev. Letters 39, (1977) 526.
(20) L. N. Bogdanova et al., Annals of Phys. 84, (1974) 261; for a review see: T. E. O. Ericson in 3° European Symp. on Antinucleon-Nucleon Interactions, Stockholm, 1976, pag. 3.
(21) For a review see: G. F. Chew in 3° European Symp. on Antinucleon-Nucleon Interactions, Stockholm, 1976, Pag. 515.
(22) G. Veneziano, Talk given at the XII Rencontre de Moriond, March 1977, CERN Preprint TH/2311 (1977).
(23) For a review see L. Montanet, talk given at the 5° Intern. Conf. on Experimental Meson Spectroscopy, Boston, 1977, CERN preprint EP/ Phys. 77-22 (1977);
P. Benkmeiri et al., Phys. Letters 68B, (1977) 483;
C. Evangelista et al., Submitted to European Conf. on Particle Physics, Budapest, 1977, CERN preprint, EP/Phys. 77-24 (1977).
(24) Basel-Karlsruhe-CERN-Stockholm-Strasbourg experiment, Private Communication by H. Koch.
(25) From "The New World" by Saul Steinberg (Harper and Row Publishers).